VARIATION CHARACTERISTICS OF THE ANCHOR DYNAMICS TESTING SIGNAL UNDER CONDITIONS OF TENSILE LOAD

Bing Sun[1*] – Songqiuyang Zhang [1] – Sheng Zeng[2] – Deng Yuan – Zhanping Liang

[1]Institute of Urban Construction, University of South China, Hengyang 421001, China
[2]School of Nuclear Resources Engineering, University of South China, Hengyang 421001, China

Abstract:

Non-destructive testing for rock bolts in this study considers loads typical of anchors in practical engineering. The non-destructive testing experiment has been conducted for bolts under various load levels with variation characteristics of the dynamic testing signal and analyzed based on the stress wave reflection method. This research indicates that reflection signals of the fixed end section are relatively strong while reflection signals of the bottom section are relatively weak, regardless of bolt bearing loads, due to the effect of transmission, reflection and attenuation of the stress wave. The dynamic signal features obvious cycles in addition to the comparatively regular waveform in no-load cases as, with increasing load, dynamic signals become increasingly unstable while mechanical properties change in the anchor rod, anchor medium and the interface. The combination method of wavelet decomposition and multi-scale is applied to the test signal analysis to improve readability and accuracy of the signal. This research indicates that wavelet analysis interacts with non-stationary signals effectively, creating a solution for the reducing signal-noise ratio caused by the load. Obviously, it can also additionally read out the reflected signal of the bottom section, thereby improving the accuracy of anchoring quality interpretation.

1   Introduction

Rock bolts have been widely applied due to cost efficiency, simple processing, convenient installation and construction speed [1-3], in a variety of forms including coal mine roadways, railways, subway tunnels, civil air defence, water conservancy, and building foundation [4-6]. Rapid and real-time non-destructive testing has become a key subject in geotechnical engineering [7-8]. Research into improvements in the precision of non-destructive testing evaluating quality of the rod anchor has been conducted and, following a series of research project results, certain achievements have been attained [9-13] with rare consideration of the load effect [14]. The anchor is often under the effect of loads in a

---

* Corresponding author. Tel.: 13789375298
E-mail address: sunbingzs@126.com

practical installation process and in practical engineering testing. If the load is disregarded, a significant difference will occur between the parameters and reality, resulting thus in inaccurate and unreasonable engineering practice guidance.

The non-destructive testing experiment measurement of the anchor model under varying load levels is discussed in this study. Dynamic signal changing characteristics of the anchor are analyzed under the influence of loads and then explored.

2 Theory of stress wave propagation in the bolt

Elastic stress waves expand from one medium to another with varying wave impedance. When the waves vertically arrive at the interface of two media types, a potential for disturbance is created. The wave propagates the reflective stress disturbance and transmitted stress disturbance to the two media separately, and then the reflection stress wave and transmission stress wave are formed. Assuming there is a change in the impedance plane of the anchor, the wave impedance in the top medium Z_1 can be derived as displayed in Formula (1):

$$Z_1 = \rho_1 C_1 A_1 \tag{1}$$

Where ρ_1 is the density of the top medium [kg/m³], A_1 is the cross sectional area of the top medium [m²], and C_1 is the propagation speed of the stress wave of the top medium [m/s].

The wave impedance in the bottom section medium Z_2 can be derived as displayed in Formula (2):

$$Z_2 = \rho_2 C_2 A_2 \tag{2}$$

Where ρ_2 is the density of the bottom medium [kg/m³], A_2 is the cross sectional area of the bottom medium [m²], and C_2 is the propagation speed of the stress wave of the bottom medium [m/s].

The ratio of the generalized impedance n can be derived as displayed in Formula (3):

$$n = \frac{Z_1}{Z_2} = \frac{\rho_1 C_1 A_1}{\rho_2 C_2 A_2} \tag{3}$$

Vibration of the anchor occurs at the end point when the anchor is subjected to the transient impact, and when the stress wave is formed by the vibration

spreads to the bottom section of the bolt, creating the reflection wave and transmission wave at the impedance interface. According to the continuous condition and theorem of momentum conservation [12], the reflection coefficient *F* and refractive index T may be derived as displayed in Formula (4) and Formula (5), respectively:

$$F = \frac{1-n}{1+n} \tag{4}$$

$$T = \frac{2}{1+n} \tag{5}$$

When $n = 1$, $F = 0$ and $T = 1$ are derived, the wave impedance of the two media types may be inferred as matching. When $n < 1$, $F > 0$ and $T > 1$ are derived, there is no phase difference when the wave spreads from the medium with small wave impedance into the medium with large wave impedance. When $n > 1$, $F < 0$ and $T < 1$ are derived, there are phase differences and the half wave loss when the wave spreads from the medium with large wave impedance into the medium with small wave impedance.

3 Model test

3.1 Model design indoor and production

The full bolt is referred to as M-1 with the anchor rod body built utilizing screw thread steel with 28 mm diameter, an anchor length of 2.4 m, and a length of exposed steel of 0.5 m. Cement mortar is employed for an anchoring medium with a ratio of 1:2:4 of water, cement and mortar, respectively, while the template is a 200 mm diameter PVC drain. The construction method is as follows: first needles are inserted followed by pouring the mortar into the template. Air plasma (an anchor with no mortar) is regarded as a defect anchor, and the diagram of bolt model structure is thus displayed (Fig.1).
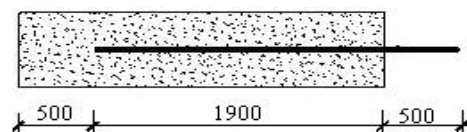

Figure 1. Structural scheme.

The stress wave reflection method produces the impact load out of the vertical vibration anchoring

bolt, signals are received by the sensor, analyzed and processed with dynamic testing analyzer.

3.2 Loading experiment and test

Centre hole jack is utilized as load material to explore the effect of different loads on the anchor. The load-step size is 10 kN according to the calculated solution with the value of strain gage measured with using the static strain meter. Signal acquisition of the anchor is processed after the strain number stabilizes during every loading period. The test system (Fig.2) is comprised of a dynamic testing analyzer as a signal analysis system, and a micro acceleration sensor. It is worth mentioning that the vertical vibration occurs first at the edge of the piezoelectric force hammer and then at the receiver sensor. The force hammer weighs 250 g with a charge sensitivity of 3.57 pC/N and it is the Lc percussion hammer produced by Lian Neng Company of Jiangsu. The dynamic signal analysis system with sampling frequency of 96 KHz is the AVANT-10 produced by Yi Heng Company of Hangzhou. Five piezoelectric acceleration transducers were utilized with frequency domains from 0.5 kHz to 10 kHz, and sensitivity of 2.47 pC/ms^2. Sampled frequency was minimally two times the highest frequency of band-limited signals to avoid folding frequency while sampling.
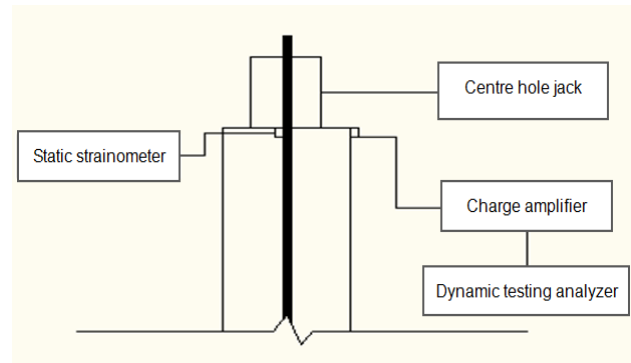

Figure 2. Test system.

4   Characteristics analysis of the original signal

Non-destructive testing of the bolt was conducted under various load levels with the acceleration response to the original signal curve of the anchor under some loading and measurable levels (Fig.3).

The signal was obviously periodical and regular under no-loading conditions according to Fig.2, with the reflection signal at the fixed end section especially strong and, at the anchor bottom, so subdued that it may not be detectable. The signal was not periodical and regular if the loading gradually increased.
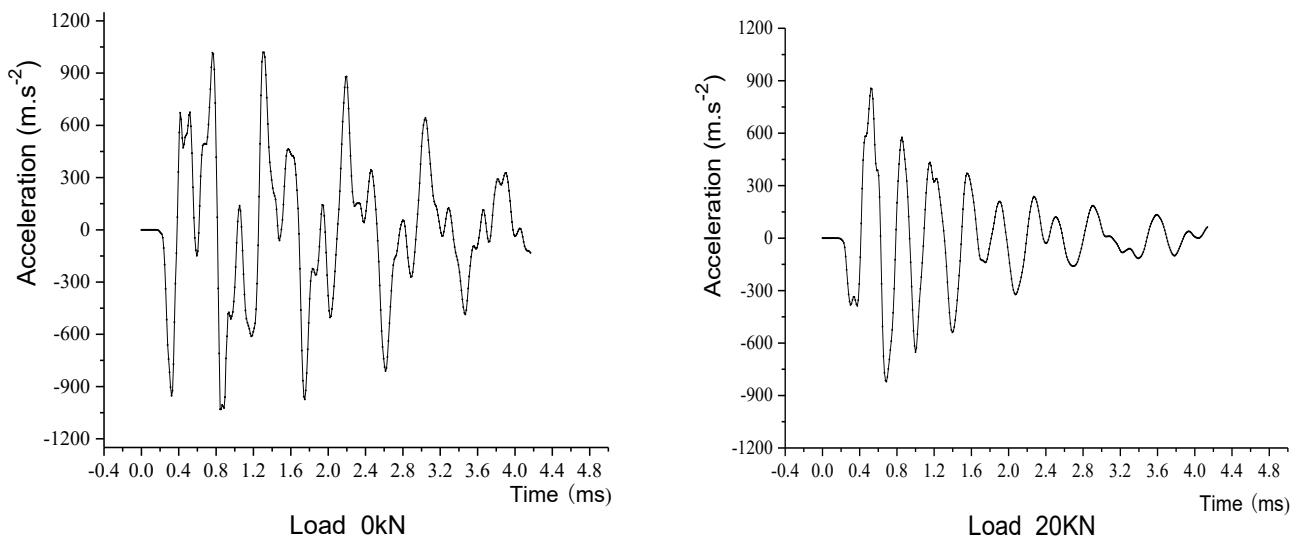

Figure 3. The original dynamic testing signals of bolt under various load levels.
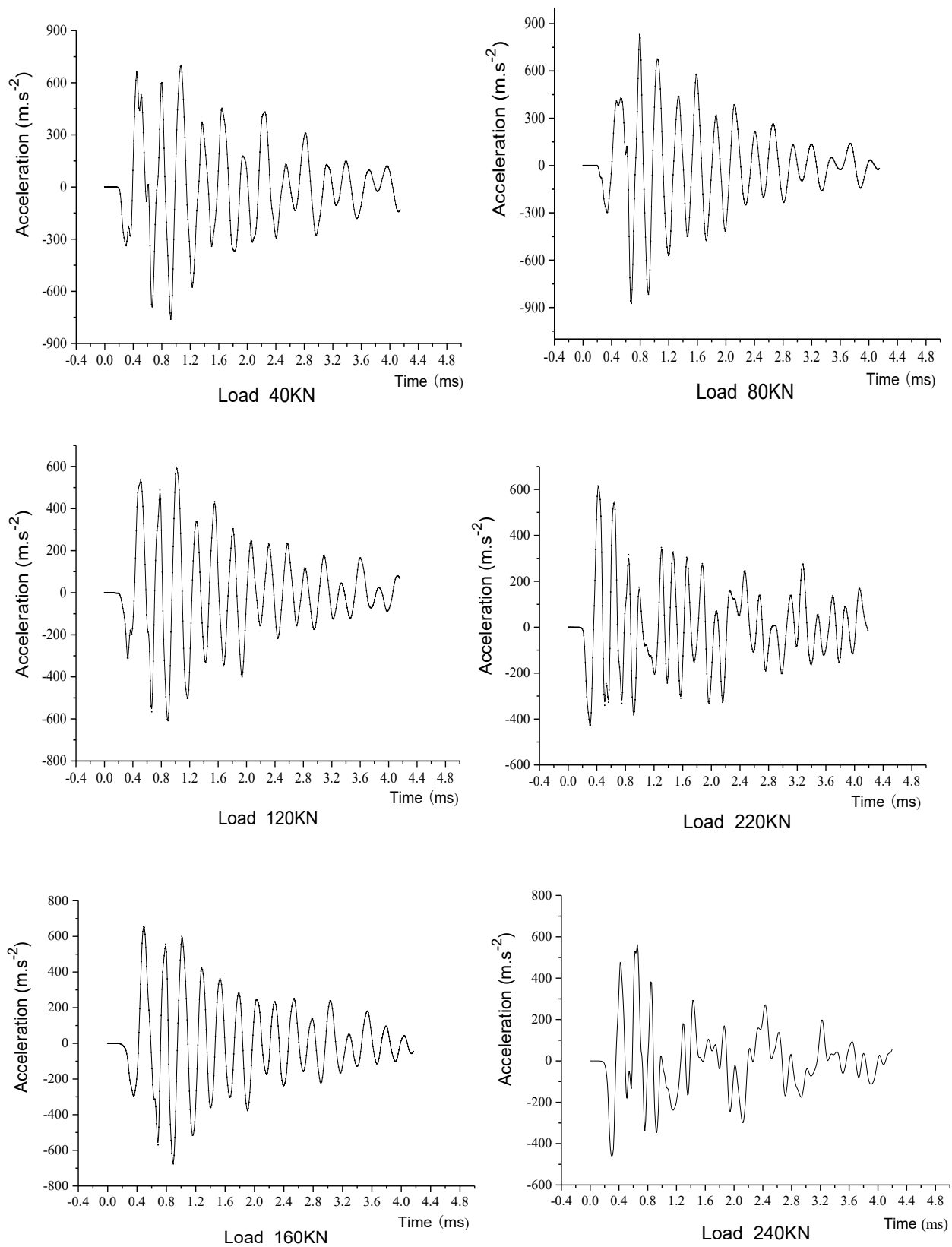
Figure 3. The original dynamic testing signals of bolt under various load levels (continued).

Compared with the amplitude of the first wave, the reflection at the fixed end section of the anchor was weaker, while the reflection at the bottom section was stronger; however, the reflection was still difficult to figure out at the anchor bottom.

The signal features changed as a result of several events: once wave impedance had altered, reflection and transmission waves were affected with the value of the amplitude and wave impedance closely related. Material properties and the cross section areas of the anchor at the fixed end section may change dramatically so that the reflection signal was very strong at the fixed end section, while the bottom section reflection signal was weak, as it was overwhelmed by the reflection signal at the fixed end section. Stress waves reached the anchor additionally and may have caused the body wave due to coupling between the medium and around the anchor. Energy then diffused and scattered to the around medium and was even absorbed; so, the stress wave continuously weakened as long as the propagation distance increased. Minimal change in the wave impedance of the anchor occurred before loading, due to the adequate joint between the anchor and the medium, and signal regularity was thus sufficient. Sliding failure occurred in some parts of the interface, with a slight relative displacement between the parts as loading increased. The signals became increasingly more complex and unstable when the anchor rod, anchor medium and mechanical properties of the interface were altered by gradual loading.

5 Wavelet analysis of the signal

5.1 The basic principle of the wavelet analysis

The wavelet analysis is designed to decompose the original signal into a series of primitive signals with clear frequency localization. Local characteristics of the original signal can be derived through analysis of various characteristics of the primitive signal so as to analyze the signal locally. A wavelet transformation of the signal is the projection on a wavelet function cluster set generated from the wavelet basis function by the scale transformation and iterative arithmetic. Wavelet basis function is referred to as the wavelet function [15-16]. Assuming the function of the signal to be analyzed is $f(t)$, the basis wavelet function $\varphi(t)$ should meet the conditions displayed in Formula (6):

$$C_\varphi = \int_{-\infty}^{+\infty} \frac{|\psi(t)|^2}{|t|} dt < \infty \qquad (6)$$

Where $\psi(t)$ is the Fourier transformation of $\varphi(t)$, and t is the variable of time [s].

The wavelet transformation of the signal $W_\varphi f(a,b)$ is displayed as Formula (7):

$$W_\varphi f(a,b) = \frac{1}{\sqrt{|a|}} \int_R f(t)\varphi(\frac{t-b}{a})dt \qquad (7)$$

Where a is the scale factor, b the translation factor, and t is the variable of time [s].

$\varphi_{a,b}(t)$ is wavelet function cluster displayed as Formula (8):

$$\varphi_{a,b}(t) = \frac{1}{\sqrt{|a|}} \varphi(\frac{t-b}{a}) \qquad (8)$$

Where a is the scale factor, b the translation factor, and t is the variable of time [s].

The function of the original signal $f(t)$ may be accurately reconstituted by its wavelet transformation $W_\varphi f(a,b)$ and may also be simultaneously regarded as decomposed according to the matrix base $\varphi_{a,b}(t)$. The original signal is not linearly independent among the matrix base $\varphi_{a,b}(t)$ as a and b varied continuously. So, in order to avoid redundancy, bases should be discreted to construct a frame. No redundancy exists when the telescopic translation system of a wavelet function is an orthogonal system since the Mallat pyramidal reconstruction algorithm can be then introduced to avoid redundancy.

The Mallat pyramidal reconstruction algorithm allows the original signal to be dispersed into a low frequency a_1 and a high frequency d_1. Low frequency a_1 may then be gradually dispersed into low frequency a_2 and high frequency d_2, in this role a_3, a_4, d_3, d_4 and so on can be got successively, indicating that any signal may be decomposed into different frequency bands. The frequency bands do not overlap and fill the whole frequency space in different decomposition layers meaning that orthogonal time-frequency windows of the discrete wavelet transformation did not overlap but individually formed a subdivision to the pair frequency plane. Energy can be counted utilizing the Mallat pyramidal reconstruction algorithm in the time domain on different frequency bands. This method is different from utilizing Fourier transform in the frequency domain. It reflects that the wavelet analysis has the advantage of providing the time-frequency analysis [17]. Time-frequency analysis, on the other hand,

provides the wavelet analysis an advantage of accuracy.

5.2 The wavelet decomposition of anchor signals

Analysis of anchor original signals under different load levels indicated extremely weak reflection signals of the bottom section regardless of load. Besides, readability of signals was reduced and the waveform became irregular as load increased with a direct influence on results in this situation. Measured signals with load under 50 kN should then be processed through the wavelet analysis so as to accurately judge the quality of the anchor.

Considering time-frequency window size, computing complexity and approximation of the base wavelet, the Daubechie wavelet may be applied to the wavelet transformation due to its advantage (with the capability) of localizing the time and frequency domain, thus allowing for a more practical digital filter. According to the waveform characteristics and frequency characteristics of the db$N$ wavelet and scaling function, the length of the filter varies as long as the value of N varies. The smoother the waveform function, the higher the value of N, and consequently the better filter frequency characteristics are; however, calculation complexity increases dramatically as long as the value of N increases. So, the db6 wavelet can be rendered. Unknown white noise should be chosen to avoid the appearance of decomposed signals as singular throughout. After performing analysis and processing of signals using

the MATLAB wavelet toolbox, the transforming solution may be obtained as displayed in Fig.4.

Conclusions may be derived from Fig. 3 as, according to the principle of wavelet transforming, the original signal S can be gotten as Formula (9):

$$S = a_4 + d_4 + d_3 + d_2 + d_1 \qquad (9)$$

The waveform of low frequency signal a_4 is regular as presented in Fig. 3, indicating no large-scale defect in the anchor. d_1 is the high-frequency signal with a low amplitude and may possibly affect individual points of the original signal. Signal change in the multiscale analysis is reflected where the intensity of signal is less defined. Wavelet analysis for ideal signals in multiscale allows different frequencies to reflect varying scales of defect while different colors correspond to varying degrees of defects with a bit shallower colour representing a more substantial defect. Multiscale analysis of signals reveals no load if the incoming signal is strong and the reflection signal is weak so that the anchor features consequently no conspicuous defects. Vibration frequency of the anchor increases providing the load increases. Denoising effect of the wavelet is obvious provided the curve becomes uniformly smooth using analysis with the bottom section reflection signal. Clearly, this signal becomes legible after decomposition without regard to load. Denoising then provides ability to assess overall quality of the anchor analysis method.
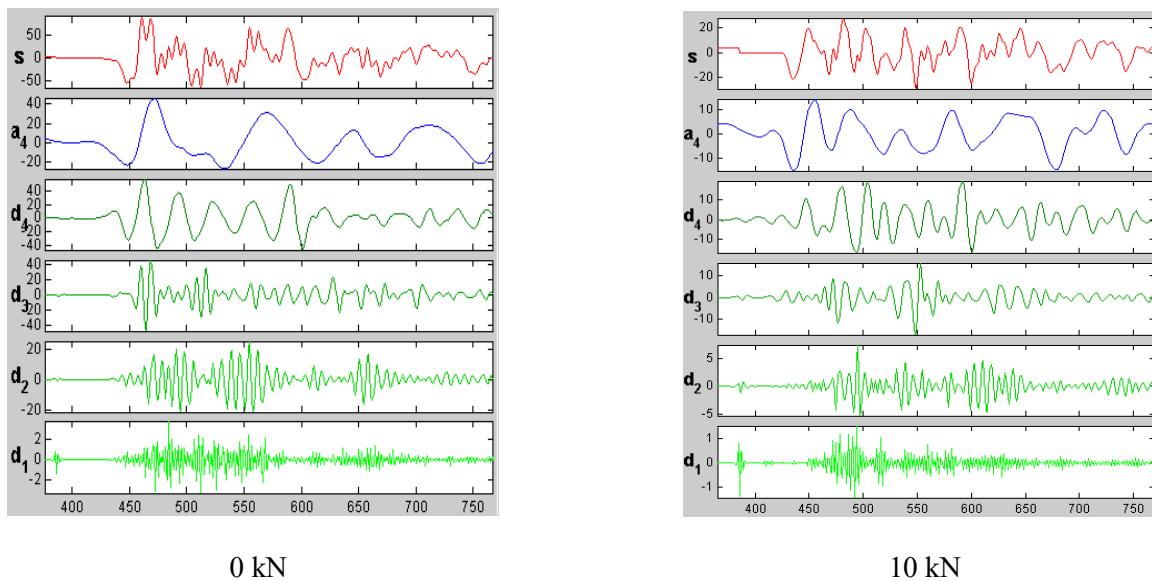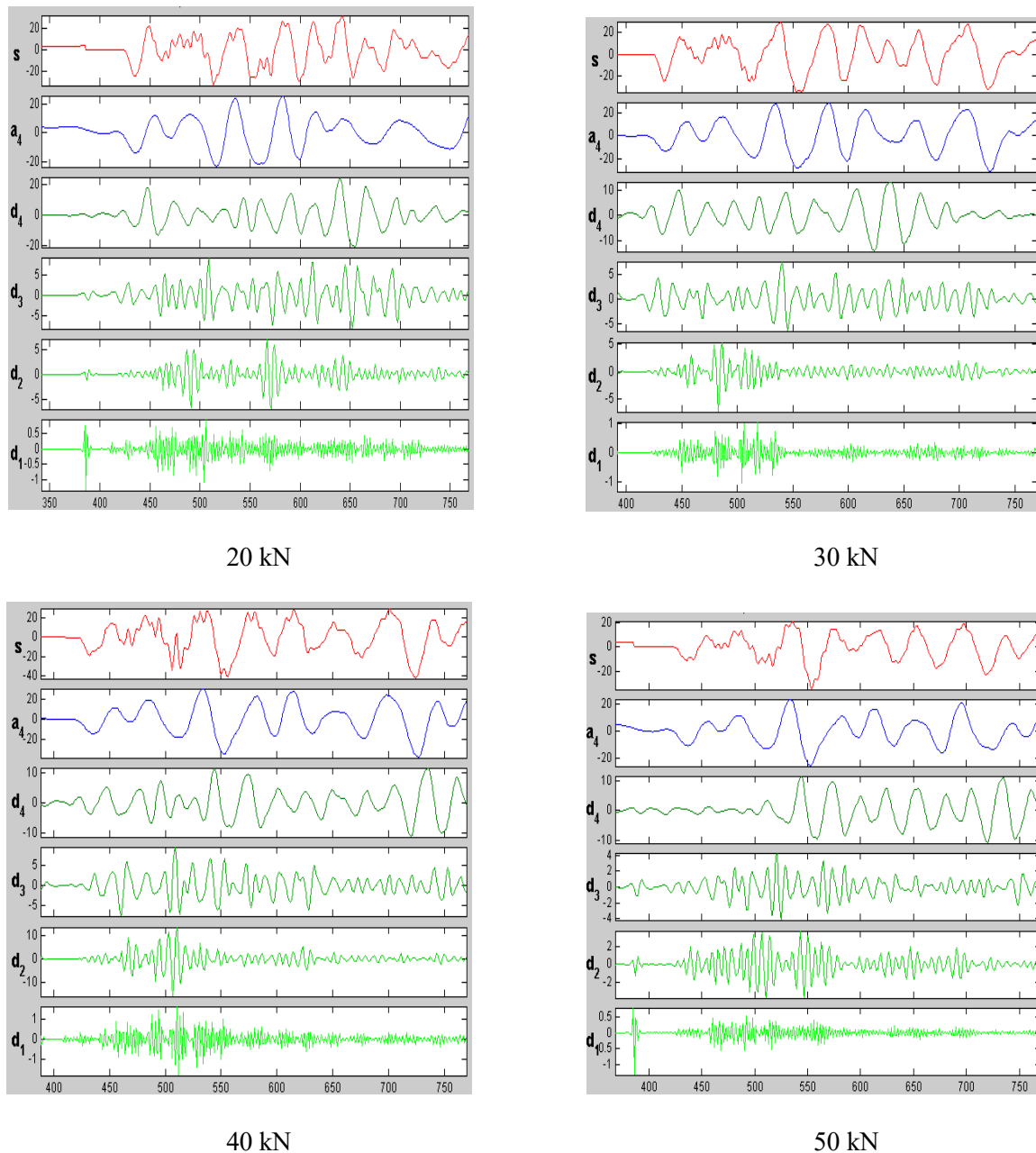

0 kN   10 kN

Figure 4. The decomposition diagrams of original signal wavelet under different levels of load (The Y-axis is the amplitude of acceleration (m/s²), the X-axis is time (ms).

20 kN

30 kN

40 kN

50 kN

Figure 4. The decomposition diagrams of original signal wavelet under different levels of load
(The Y-axis is the amplitude of acceleration (m/s²), the X-axis is time (ms) (continued).

6   Conclusions

(1) Reflection signal of the fixed end section original signal is strong regardless of load; however, reflection signals of the bottom section are weak and difficult to figure out. Compared with the amplitude of the first wave, by increasing the load/with an increase in load, reflection at the fixed end section weakens, while reflection of the anchor at the bottom section becomes stronger.

(2) The waveform curve is obviously periodical and regular with no load; provided the load increases, periodical nature of the curve becomes tenuous while waveform irregularity increases.

(3) The amplitude of the vibration signal increases with an increasing load. Smoothness of the original signal is then affected and the signal-noise ratio reduces simultaneously. As long as load increases, the original signal waveform becomes irregular and then it is difficult to have a conclusion only through analyzing an original signal. So, testing anchor

quality features disadvantages only through the original signal analysis. Wavelet theory application improves reflection signal legibility of the bottom section by improving overall accuracy of the anchor quality.

Acknowledgments

References

[1] Kang, H., Cui, Q., Hu, B., et al.: *Analysis on anchorage performances and affecting factors of resin bolts*, Journal of China Coal Society, 39 (2014), 1, 1-10.

[2] Wang, G., Liu, C., Wu, X..: *Coupling rheological model for end-anchored bolt and surrounding rock mass*, Chinese Journal of Geotechnical Engineering, 36 (2014), 2, 363-375.

[3] Wu R., Xu J., Li C., et al.: *Stress wave propagation in supporting bolts: a test for bolt support quality*, International Journal of Ming Science and Technology, 22 (2012), 4, 567-571.

[4] LIU, H., Wang, F., Jiang, L., et al.: *On the performance of lengthened bolt coupling support system in roadway roof,* Journal of Mining & Safety Engineering, 31 (2014), 3, 366-372.

[5] Shan, R., Kong, X., Wei, E., et al.: *Theory and application of strong support for coal roadway sidewall*, Chinese Journal of Rock Mechanics and Engineering, 32 (2013), 7, 1304-1314.

[6] Xue, D., Wu, Y., Zhang, K..: *Experimental study and application on non-destructive testing of bolt axial force in coal mine*, Journal of Mining & Safety Engineering, 30 (2013), 3, 375-379.

[7] Yang, T. C., Wu, Y., Xia, D.: *An analytic method for rock bolt's non-destructive testing signals by phase deducted method*, Journal of China Coal Society, 34 (2009), 5, 629-633.

[8] Zou, D. H., Cui, Y., Madenga, V., et al.: *Effects of frequency and grouted length on the behavior of guided ultrasonic waves in rock bolts*, International Journal of Rock Mechanics & Mining Sciences, 40 (2007), 813- 819.

[9] Li, Y., Zhang, C., Wang, C.: *Study on several key issues in nondestructive detection of bolt bonding integrality,* Chinese Journal of Rock Mechanics Engineering, 27 (2008), 1, 108-116.

[10] Zhang, C. S., Zou, D. H., Madenga, V.: *Numerical simulation of wave propagation in grouted rock bolts and the effects of mesh density and wave frequency*, International Journal of Rock Mechanics & Mining Sciences, 43 (2006), 634- 639.

[11] Beard, M. D., Lowe M. J. S.: *Non-destructive testing of using guided ultrasonic waves*, International Journal of Rock Mechanics and Mining Sciences, 40 (2003), 527–536.

[12] Wang, M., Wang, H.: *Nondestructive testing of anchoring quality,* Chinese Journal of Rock Mechanics and Engineering, 21 (2002), 1, 126 - 129.

[13] Chen, J., Hu, J., Zhang, Y.: *Identification of surrounding rock quality based on dynamic testing technology of integrated anchor*, Rock and Soil Mechanics, 30 (2009), 6, 1799-1804.

[14] Li, Y., Liu, H., Wang, F.: *Nondestructive testing of parameters of bolt anchoring state and its application*, Chinese Journal of Rock Mechanics and Engineering, 23 (2004), 10, 1741-1744.

[15] Ren, Z., Li, Y.: *Analysis of detection signal and realization on evaluation system of bolt anchoring quality based on sound wave testing*, Journal of China Coal Society, 36 (2011), 1, 191-196.

[16] Sun, B., Zheng, X., Zeng, S., et al.: *Multi-scale analysis on anchoring defects diagnosis under multiple measuring points*, Journal of China Coal Society, 33 (2014), 3, 305-310.

[17] Avdakovic S., Bosovic A., Hasanspahic N., et al.: *Time-frequency analyses of disturbances in power distribution systems,* Engineering Review, 34 (2014), 3, 175-180.